Engineered Science
DOI: https://dx.doi.org/10.30919/es927

On the Development of a Passive Shape Memory Alloy- Based Cooling System – Part I: Design and Implementation

Aniello Riccio,[1] Andrea Sellitto,[1,*] Domenico Borrelli,[2] Raffaele Sansone,[2] Antonio Caraviello,[2] Ugo Riccio,[3] Antonio Torluccio,[3] Luca Pacini[3] and Rouven Mohr[3]

Abstract

The development of structures able to modify their shapes, according to specific conditions, is considered a future challenge for engineering applications. In this framework, the use of shape memory alloy (SMA)-based actuators is undoubtedly promising. In this paper, the development of a passive SMA-based actuator, for automotive application, produced with the aid of additive manufacturing technologies, is presented. The actuator is passively controlled by the temperature reached in the engine compartment. Indeed, the increase of temperature beyond a predetermined threshold trigger, by means of the SMA-based actuator, a set of cooling flaps which dissipate the heat accumulated in the engine compartment. This operation is able to improve cooling performances of cars. The performed extensive development activity has been split into two parts which are presented in two papers. The present paper focuses on part I, dealing with design and manufacturing steps; while detailed finite element analyses, aimed to the numerical justification of the design of the proposed passive cooling system, are introduced in part II.

Keywords: Passive cooling system; SMA; ALM; Actuator.
Received: 20 January 2023; Revised: 09 June 2023; Accepted: 15 June 2023.
Article type: Research article.

1. Introduction

In the recent years, the demand of structures able to autonomously change their shape, according to variable environmental conditions, has unquestionably increased. As an example, adaptive external and internal aerodynamics has been found attractive for many engineering applications, mainly in aeronautical and automotive fields.[1-5] To obtain the morphing of the surfaces, needed to satisfy the aerodynamic requirements, piezoelectric and/or smart materials have been used.[6-13] Among the smart materials, Shape Memory Alloys (SMA) can be considered one of the most investigated.[14]

Shape Memory Alloys are a family of metallic materials able to restore a predefined initial configuration, after a deformation, if subjected to appropriate thermal and stress loading conditions. SMA crystals can switch from the martensitic configuration, characterized by low yield strength and high deformability (hyperelastic behaviour), to the austenitic more mechanically performant configuration, if heated above a temperature threshold.[15-17] Significant energy may be exerted, which is initially stored as atomic bonds in the martensitic phase, and then released during the transition to the austenitic phase. By means of appropriate heat treatments, it is possible to modify the transition temperature and the forces exerted by the material. Indeed, Shape Memory Alloys are particularly suitable as actuators in engineering applications, being characterized by a high power-to-weight ratio.[18,19]

Actually, Shape Memory characteristics can be also found in some polymers, which are particularly suitable for composite actuators applications. In Ref. [20], 3D printed soft polymer matrix and shape memory polymer layers were coupled to design soft composite actuators. Investigation on material shape retention and recovery was carried out by considering different shape memory polymer layer thicknesses. The deformation of the actuators was predicted

[1] *University of Campania "Luigi Vanvitelli", Department of Engineering, via Roma 29, Aversa (CE), 81031, Italy.*
[2] *Sòphia High Tech, via Romani 228, Sant'Anastasia (NA), 80048, Italy.*
[3] *Automobili Lamborghini S.p.A., Via Modena 12, Sant'Agata Bolognese (BO), 40019, Italy.*
**Email*: andrea.sellitto@unicampania.it (A. Sellitto)

by means of nonlinear finite element analyses.

A novel Variable Camber Guide Vane (VCGV) actuated by a shape memory alloy plate is investigated in Ref. [21]. Analytical and numerical models were used to investigate the SMA behaviour and to design the VCGV.

An algorithm to predict the nonlinear response of SMA-structures, aimed to support the design of smart deformable aeronautical configurations capable to achieve pre-defined target shapes, is presented in Ref. [22]. The algorithm was used in Ref. [22], in conjunction with an optimization method, to predict the optimal structural and operational parameters, according to specific target shapes requirements.

In Ref. [23], the morphing capabilities of complex active structural systems were investigated. A device, is presented, which is aimed to induce deformation in the wing regions while resisting the aerodynamic and the structural loads.

In this work, the design, development, industrialisation, prototyping, and testing of a passive engine cooling system developed using the Shape Memory Alloys technology is described. The prototype has been developed to be integrated as case study on the Rear-Bonnet of the Lamborghini Aventador S. The device takes advantages of the characteristics of Shape Memory Alloys to generate the load needed for opening the rear flaps in the engine compartment of the vehicle. Hence, a passive actuation device, totally independent from the vehicle electronic systems and with no need of any electromechanical control, has been designed. The actuation system is triggered by the heat provided by the powertrain, under operating conditions. Indeed, despite Shape Memory Alloys are a fairly well-established technology in the automotive and industrial sectors in general, the added value of this work is to be found in the use of their peculiar characteristics to develop a device aimed to the passive control of the temperature in the engine compartment which does not require a control unit. In this way, a more robust mechanical system, compared to an equivalent electromechanical or electrohydraulic handling system, can be designed, with advantages in terms of weight, complexity, and consumption reductions linked, among the others, to the more-controlled engine operative temperatures.

The activity stream follows the DMAIC (Define, Measure, Analyse, Improve, Control) approach, according to which the R&D and industrial activities can be appropriately defined to guarantee effective results. The flowchart of the performed activities is summarized in Fig. 1.

This paper, describing the part I of the performed activities, has been arranged according to the bold test boxes of the flowchart in Fig. 1: Requirements, Preliminary Design, Executive Design, Manufacturing, Assembly and Testing. Actually, the Structural FEM Analysis, the Redesign and the Topology Optimization activities, which provide a justification of the implemented design, are introduced in the part II paper.[24]

In section 2 the concept of antagonistic actuators is introduced; then, the device requirements are defined, leading to the preliminary design, as discussed in section 3. In section 4, the executive design is presented; while in section 5, the manufacturing process is detailed. Finally, in section 6, the assembly and testing operations are presented.

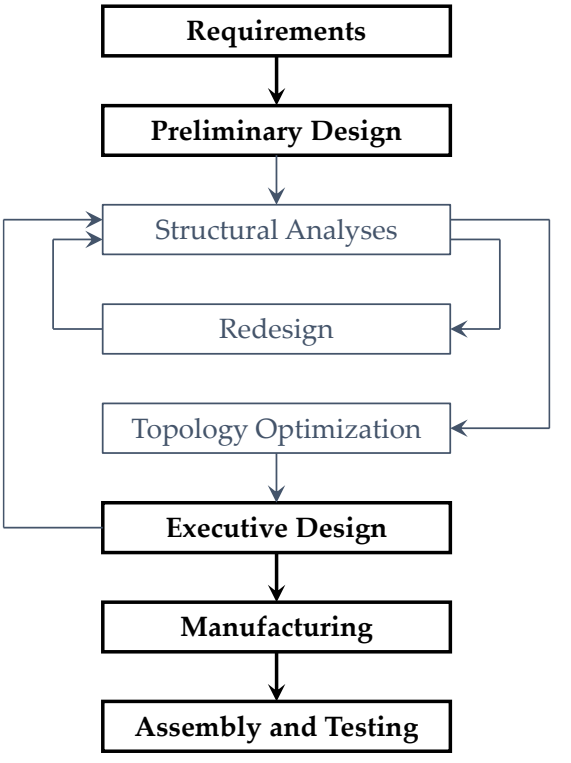

Fig. 1 Activities flowchart.

2. Antagonistic actuators

Shape memory alloys are a class of metallic materials characterised by two phases, namely the austenite and martensite: martensitic phase is considered stable at low temperatures, while the austenitic phase is stable at high temperatures (Fig. 2).

A key characteristic of SMA is their shape memory effect, which is the ability to recover the initial state after deformation has occurred when subjected to a temperature above a predefined threshold. This characteristic makes them particularly suitable for the use as actuators, as they can exert recovery forces, as well as torque or displacements, through an initial compression phase, which is intended to "load" the mechanism (stress-induced phase transition). Through subsequent heating above the phase transition temperature, the device will be released in order to achieve actuation (temperature-induced phase transition).

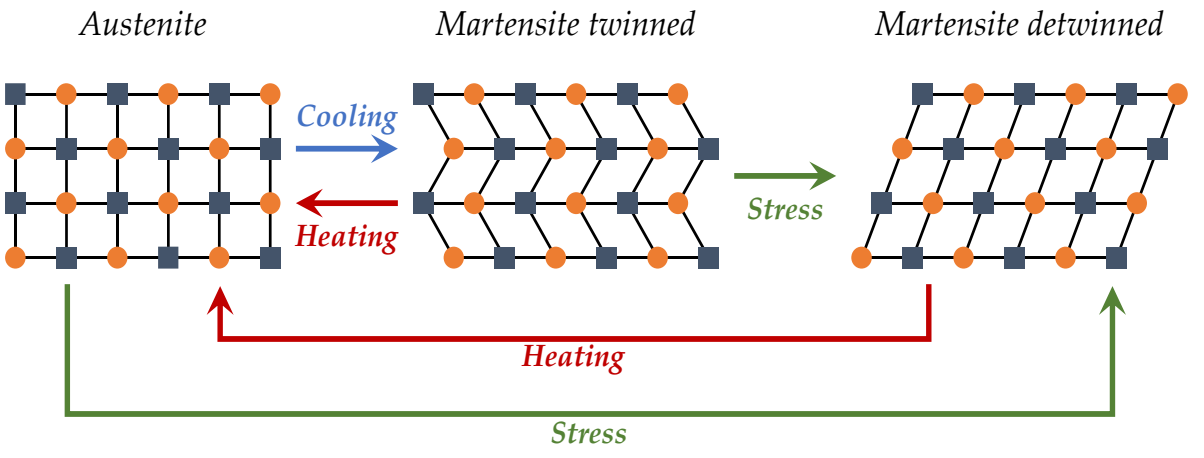

Fig. 2 SMA phases.

There are several applications in the literature that exploit the special characteristics of shape memory materials. In the recent years, the concept of antagonistic actuators has been increasingly developed, where two elastic components work in opposition to each other. In this work, an antagonistic actuator composed of a traditional Bias spring and a SMA component has been considered.

A detailed description of the mechanism can be observed in Fig. 3, where the load-displacement curves of the spring in austenitic (hot) and martensitic (cold) phases are shown in red and blue, respectively. Furthermore, the grey line AB represents the linear load-displacement curve of the bias spring. In the location A, the SMA component (in martensite phase) and the bias component are in equilibrium. However, heating the SMA results in a transition from the martensite to the austenite phase. The latter is characterized by a stiffer crystal lattice, resulting in the new equilibrium condition at location B. Since no external loads are applied, the transition from location A to location B is the maximum stroke of the actuator allowed.

If an external load is applied to the actuation system, the equilibrium condition must account the additional force as well, resulting in an intermediate final state between locations A and B. Fig. 4 shows the new equilibrium condition described by location C, in which the extra load has been exerted.

3. SMA-based cooling system preliminary design

3.1 Device requirements

The aim of the developed passive cooling system is to lower the temperatures inside the engine compartment and at same time guarantee aerodynamic performances avoiding permanent holes under the wing. Hence, the device consists of a kinematic mechanism able to self-actuating as soon as a predetermined temperature is reached in the engine compartment. Fig. 5 shows the modified rear-bonnet and its location on the Aventador S car model.

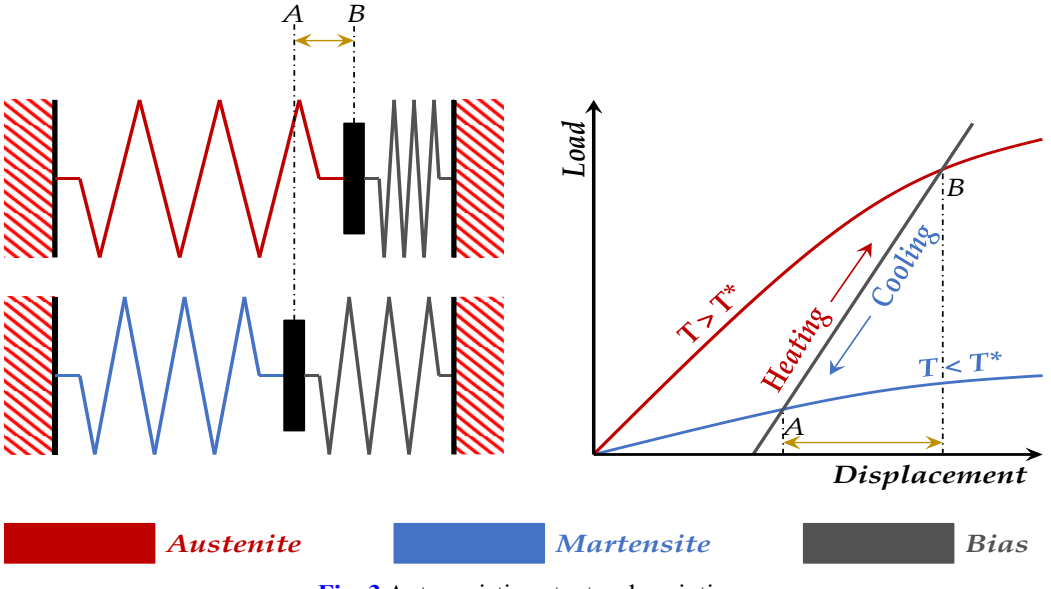

Fig. 3 Antagonistic actuator description.

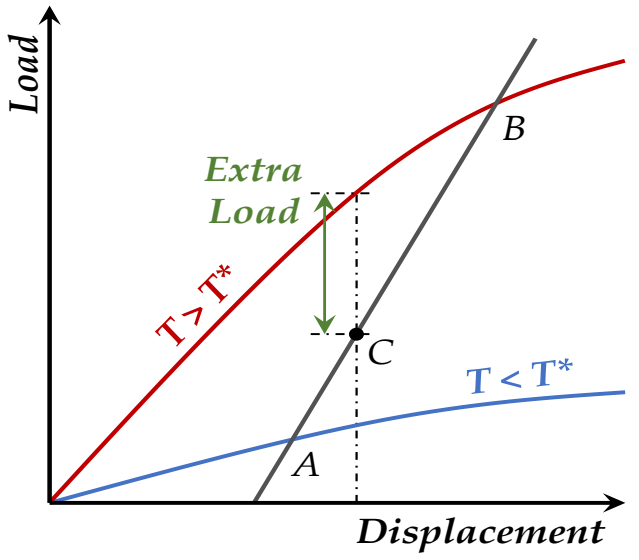

Fig. 4 Antagonistic actuator with external load.

The six rear flaps remain closed in all the car driving conditions, since the cooling induced by the vehicle air intakes keeps the temperature in the engine compartment below the SMA activation threshold. However, investigations on thermal behaviour of engine compartment demonstrated that during heat soak condition, underhood engine compartment temperature raises. To avoid these circumstances, different solutions could be chosen. Among the others, the most common is to open some holes above muffler, which impacts on overall downforce of the vehicle. In this case, in a complete autonomous way, the six rear flaps open and allow the hot air to leave the engine compartment only when needed, with a consequent temperature decrease. From temperature measurements in the engine compartment and, in particular, at SMA location, a SMA activation temperature $T_{activation}$ has been found the best compromise, taking into account all the driving conditions, for triggering the opening of the rear flaps. When temperature at SMA location decreases under the activation threshold, the transformation of SMA actuator to its martensitic condition allows the rear flaps to return to their initial closed position. Moreover, in the considered temperature $T_{activation}$ range, the effect of the hysteresis can be considered negligible, since it minimally affect the load exerted by the actuation system.

The SMA actuators should be able to withstand the aerodynamic loads on the rear flaps, during the fast car restart, until temperatures in the engine compartment falls under the SMA activation threshold. To correctly design the handling system and to calibrate the maximum loads acting on the kinematic mechanism, preliminary aerodynamic analyses have been carried out on the entire car. Conservatively, the most critical conditions, corresponding to the car traveling at about 350 km/h (with flap closed), have been considered for the evaluation of the aerodynamic loads acting on the full opened rear flaps (rotation of 60°). The results of these preliminary analyses are summarized in Fig. 6.

It is worth to mention that, as a consequence of the aerodynamic loads acting on the rear flaps, the proposed solution seems to be particularly effective if compared to an electromechanically actuated device. Actually, the electric motors should be dimensioned to deliver a torque capable of overcoming the aerodynamic moment under the most severe conditions. The consequent electric motor sizing could not comply with the available space restrictions related to the current design of the Rear Bonnet and the existing components of the engine compartment.

3.2 Preliminary design

According to the SMA device requirements and to restrictions related to its location, a first preliminary design of the cooling system has been attempted. The proposed design considers six flaps activated by a spring/spring actuation system consisting of shape memory (SMA) and conventional (bias) springs.[25,26] A transmission device is used to transfer the loads from the

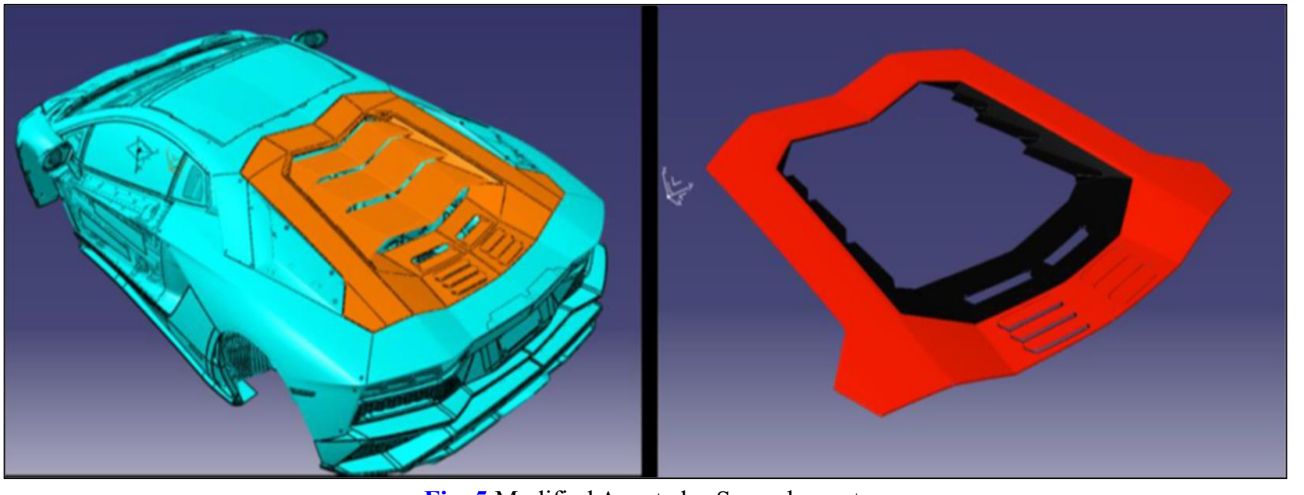

Fig. 5 Modified Aventador S rear-bonnet.

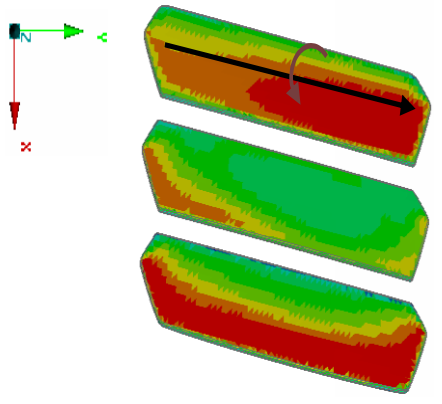

60° orientation

	$\frac{\lvert F\rvert}{\lvert F\rvert_{MAX}}$	$\frac{F_x}{\lvert F\rvert_{MAX}}$	$\frac{F_y}{\lvert F\rvert_{MAX}}$	$\frac{F_z}{\lvert F\rvert_{MAX}}$	$\frac{M}{M_{MAX}}$
Flap #1	0.781	0.622	-0.099	-0.462	0.795
Flap #2	0.214	0.167	-0.025	-0.131	0.444
Flap #3	1.000	0.778	-0.113	-0.617	1.000

Fig. 6 Aerodynamic loads acting on the 60° opened flaps.

SMA actuation system to the flaps. The preliminary designed cooling system is shown in Fig. 7. As already mentioned, one of the main restrictions for the cooling system device is related to the available space for installation. Indeed, the device must fit into a reduced working volume (the area below the rear bonnet), respecting all the pre-existing layout constraints.

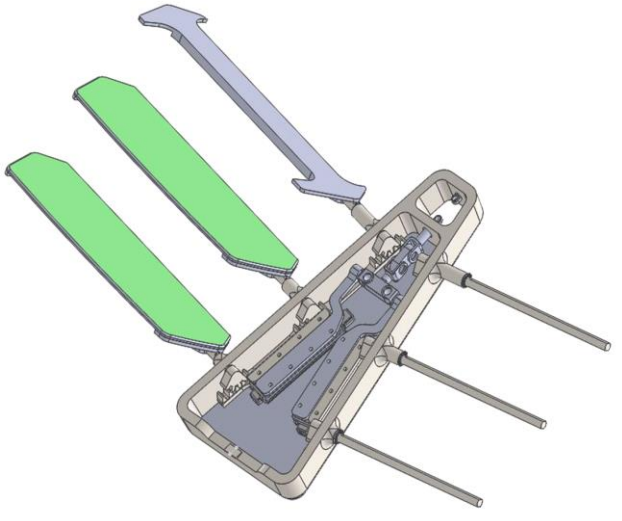

Fig. 7 Preliminary design of the SMA-based cooling system device.

Additional constraints must be considered, related to the limited deformation/load combination range of the SMA springs, used to induce the rotation on the flaps. Therefore, an ad-hoc gear system has been developed, consisting of customised cogwheels and gear racks. This system is mechanically connected to the SMA spring actuation system via a transmission rod, drilled at one end to allow the connection to the SMA actuation system, as shown in Fig. 8. Due to the reduced dimensions of the assembly, no commercially available standard components were identified; hence, custom design and manufacturing of all the internal components of the mechanisms was needed. Each gear rack is coupled with three custom gears (one for each flap) which allow the actuation of the flaps through a rotating axis. This rotating axis is coupled inside a location in the flap support and secured by an M3 grub screw. Initially, 1.5 mm pitch gears were used to achieve the required 60° opening angle for the flaps. However, since the maximum allowable stroke of the SMA springs was 5 mm (due to space constraints), the pitch was subsequently reduced to 0.5 mm.

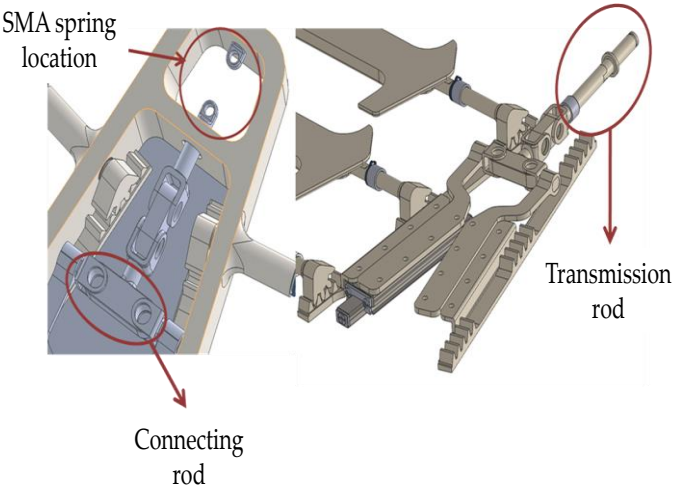

Fig. 8 SMA spring location and transmission mechanism.

The manufacturing of such mechanisms using Computerized Numerical Control (CNC) technology is a very delicate and complex task. To speed up the prototyping and production phases, the system was redesigned, oriented to the additive manufacturing technology. A linear guide composed by slide and rail was introduced to prevent friction between the surfaces during operation. In Fig. 9 the gear rack and the linear guide are shown, while Fig. 10 reports the flap support and the rotation rod with the custom gear.

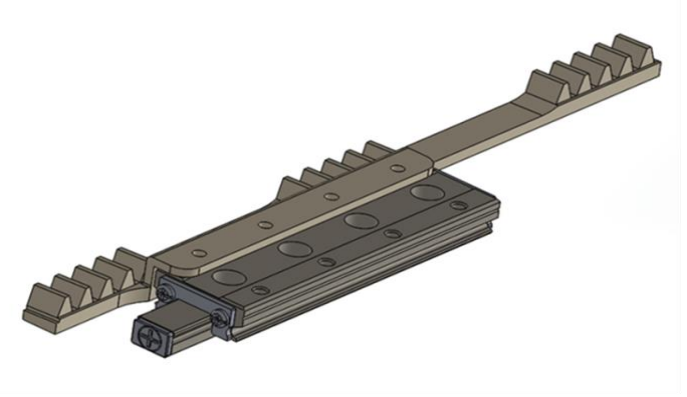

Fig. 9 Gear rack and linear guide.

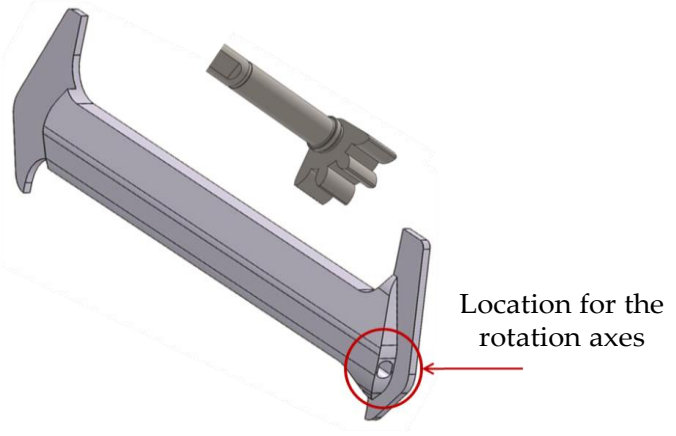

Fig. 10 Flap support and rotation rod.

To achieve the desired actuation load for the mechanism, four SMA springs and four bias springs have been considered, as shown in Fig. 11. This choice allowed to keep the SMA maximum allowable stroke below 5 mm.

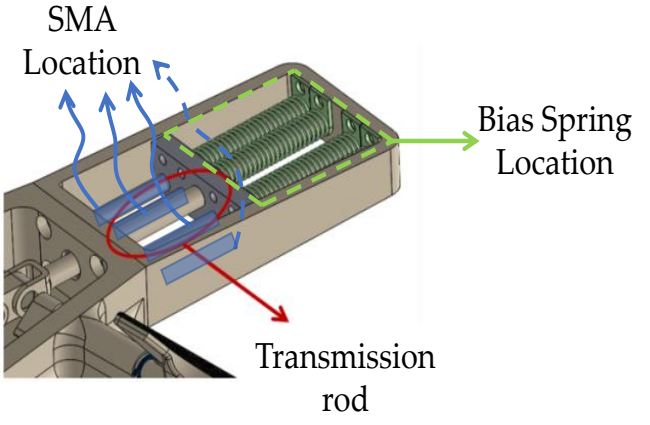

Fig. 11 SMA spring assembly frame design.

To verify the kinematics, firstly, a CAD model was created; then, a physical mock-up was manufactured by using PLA by a Fused Deposition Modelling (FDM) 3D printing process. Fig. 12 shows the physical mock-up, while details of the 3D printed SMA spring assembly are reported in Fig. 13.

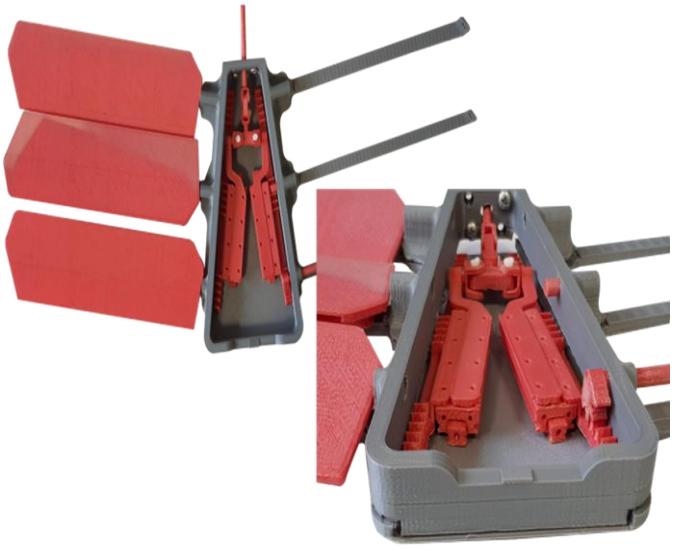

Fig. 12 PLA physical mock-up.

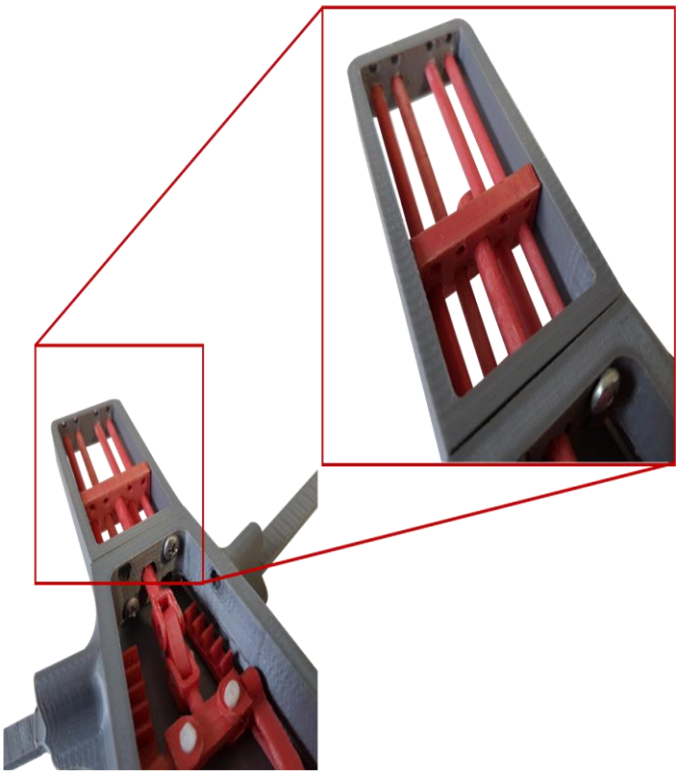

Fig. 13 PLA physical mock-up: detail of the SMA spring assembly frame.

After the issue of the initial preliminary concept definition, the SMA-based cooling system device experienced several redesigns to comply to the functional requirements, according to the flowchart in Fig. 1. In this redesign phase, strong modifications have been made to the spring assembly. In Figs. 14 and 15 the final configuration before topology and weight optimization is shown. According to this configuration, the SMA and bias spring have been positioned in parallel to save space under the rear bonnet location. A central section with four SMA springs characterised by 16 mm and 11 mm external

and internal diameters, respectively, and two additional lateral section accommodating four bias springs, each characterised by 15 mm and 12 mm external and internal diameters, respectively. In Fig. 14 a detailed view of the spring assembly is presented.

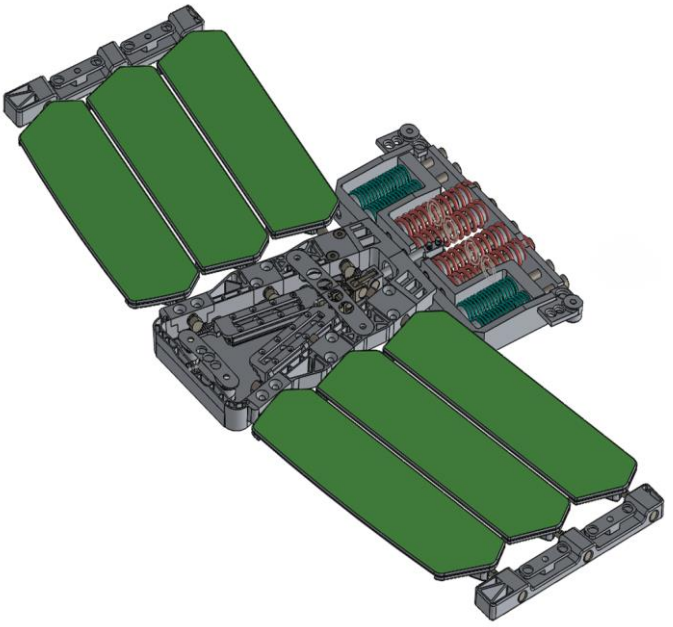

Fig. 14 SMA- based cooling system device - Final configuration before topology and weight optimization.

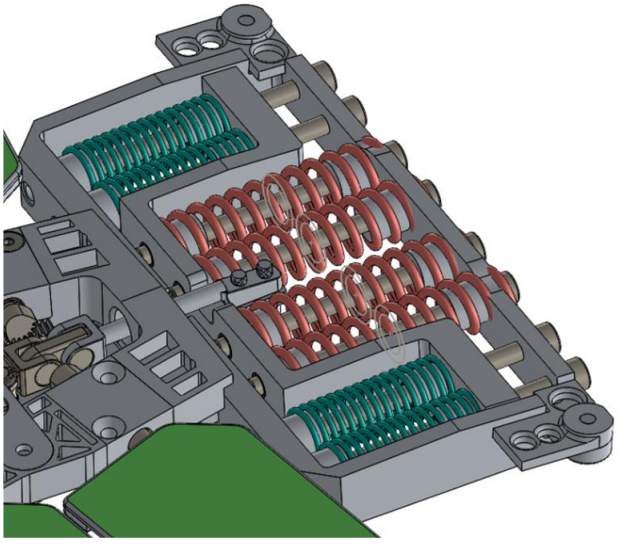

Fig. 15 Spring assembly component - Final configuration before topology and weight optimization.

In Figs. 16 and 17 the fixing brackets, used for connecting the entire system to the rear bonnet, are shown. The fixing brackets are located on the side support (Fig. 16) and on the crankcase of the device (Fig. 17). Eight attachment points have been used to connect the SMA-based cooling system device to the Lamborghini Aventador S body.

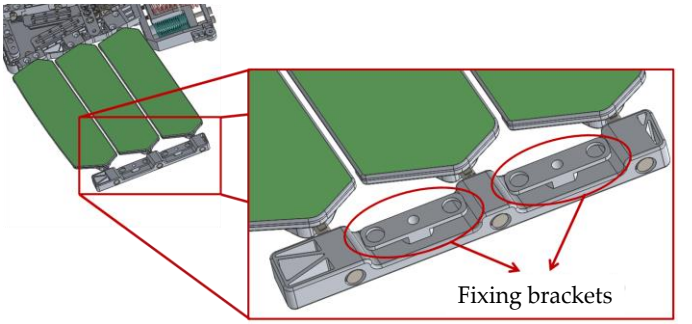

Fig. 16 Fixing brackets on the side support.

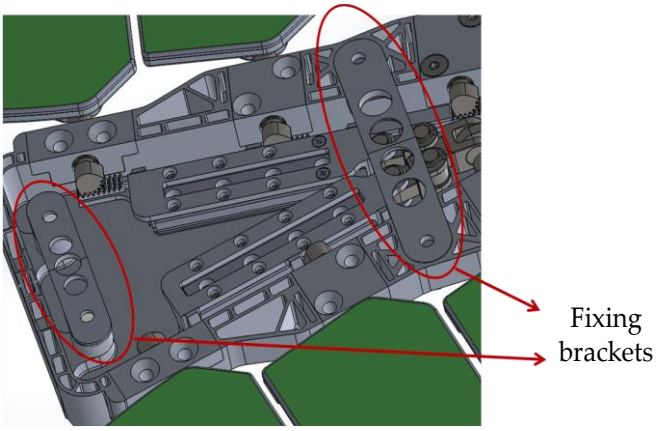

Fig. 17 Fixing brackets on the crankcase.

4. SMA-based cooling system executive design

According to Fig. 1, Numerical Structural Analyses and topological/weight optimization activities have been performed to define the final executive design of the SMA-based cooling system device. These activities, for the sake of brevity, are omitted in this paper, since they are extensively presented in the part II paper, focused on the numerical design justification activities.

The final executive design of the SMA-based cooling system device can be seen as the assembly of two macro-groups of components, arranged according to component complexity and, therefore, adopted manufacturing technology. For conventionally manufactured components, CNC (Computerized Numerical Control) manufacturing technology has been used (milling and turning), while particularly geometrically complex components have been manufactured by employing the ALM (Additive Layer Manufacturing) process. Additionally, specific components have been manufactured by ALM and, subsequently, refined by adopting numerical controlled milling.

The design process for each component considered the adopted manufacturing technology characteristics to improve the weight saving and reduce the space needed by the proposed device.

The ALM printed components have been designed considering excess metal in the regions in contact with the

manufacturing plate (where the selective laser melting is performed) and with the functional surfaces (i.e., the surfaces in contact with other components) to facilitate the CNC refining phases and to allow the detachment of the printed component from the manufacturing plate by using electrical discharge machining.

The real total device weight can be obtained by the summation of the components weights, equal to 1257.6 g, increased by adding the weight of the commercial standard pieces used for the device, such as bushings, bearings, circlip, bolts, linear guides, and connecting rod pins. The real total weight of the device is 1630 g.

As for the previous designed configurations, four SMA springs and four conventional steel bias springs have been used to satisfy the requirements in terms of actuation load. The SMA-BIAS system has been designed and calibrated with a bias springs load able to guarantee the closed condition in the presence of accidentally hand actions on the rear flaps. Then, as the temperature in the engine compartment increases, the force exerted by the SMA springs increases and overcomes the antagonistic force exerted by the bias springs plus the aerodynamic loads, leading to the rear flaps rotation and, then, to the engine compartment opening.

5. SMA-based cooling system manufacturing

In this section, the manufacturing process of the SMA-based cooling System device components is described. As already remarked, the components of the passive cooling system have been manufactured by using the traditional process, the ALM process, and a combination of them, as detailed in the following subsections.

5.1 CNC milling process

Indeed, no appreciable advantages can be expected by ALM technologies when manufacturing very small and geometrically simple components; hence, these components have been manufactured by using a standard CNC milling process. As examples of standard CNC milled components, images of the spring assembly frame pt. 2, the connecting rod #1, and the fixing brackets on the crankcase are, respectively, shown in Figs. 18-20.

5.2 ALM process

Components characterized by complex geometries and lightening openings have been manufactured by using ALM technology. These components have been appropriately designed to ensure the best combination of mechanical strength and weight reduction. As already mentioned, some of these components have been refined with CNC. Examples are shown in Figs. 21 and 22, which reports respectively the crankcase and the lateral supports.

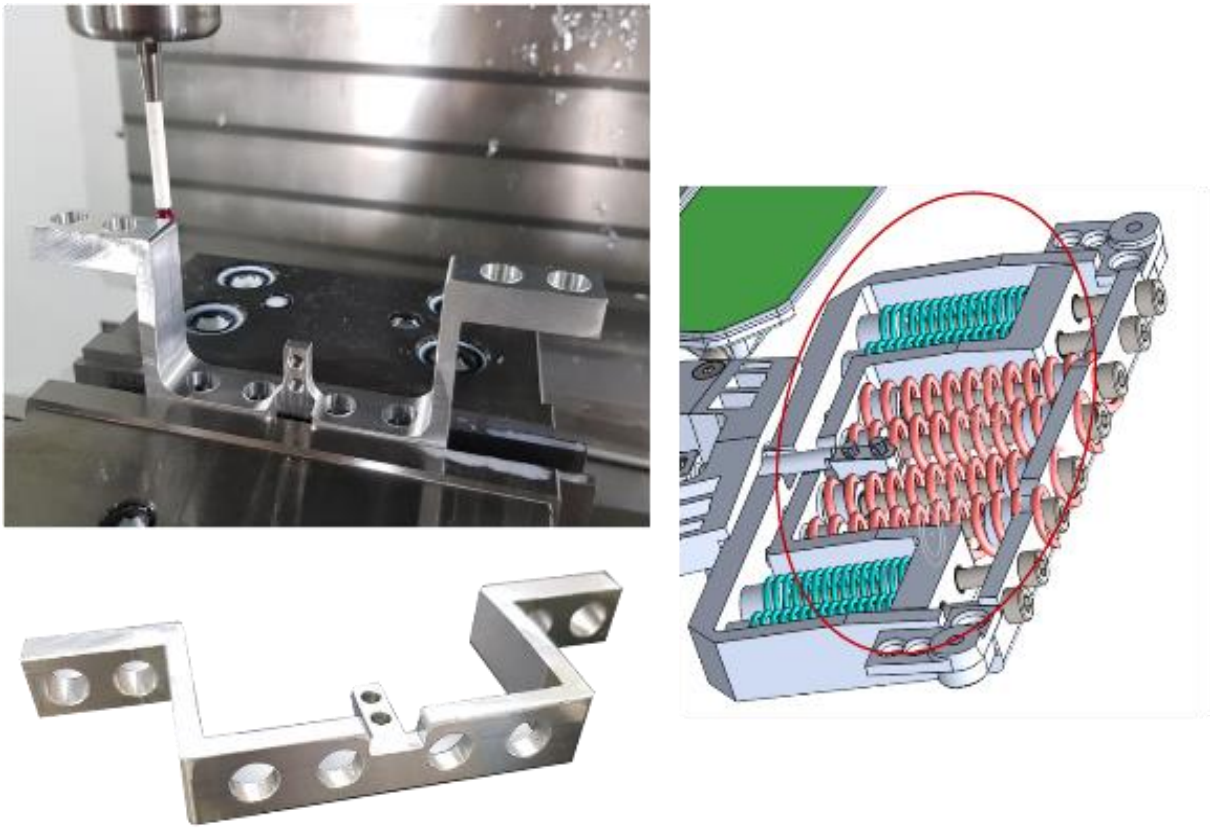

Fig. 18 CNC manufacturing of the spring assembly frame pt. 2.

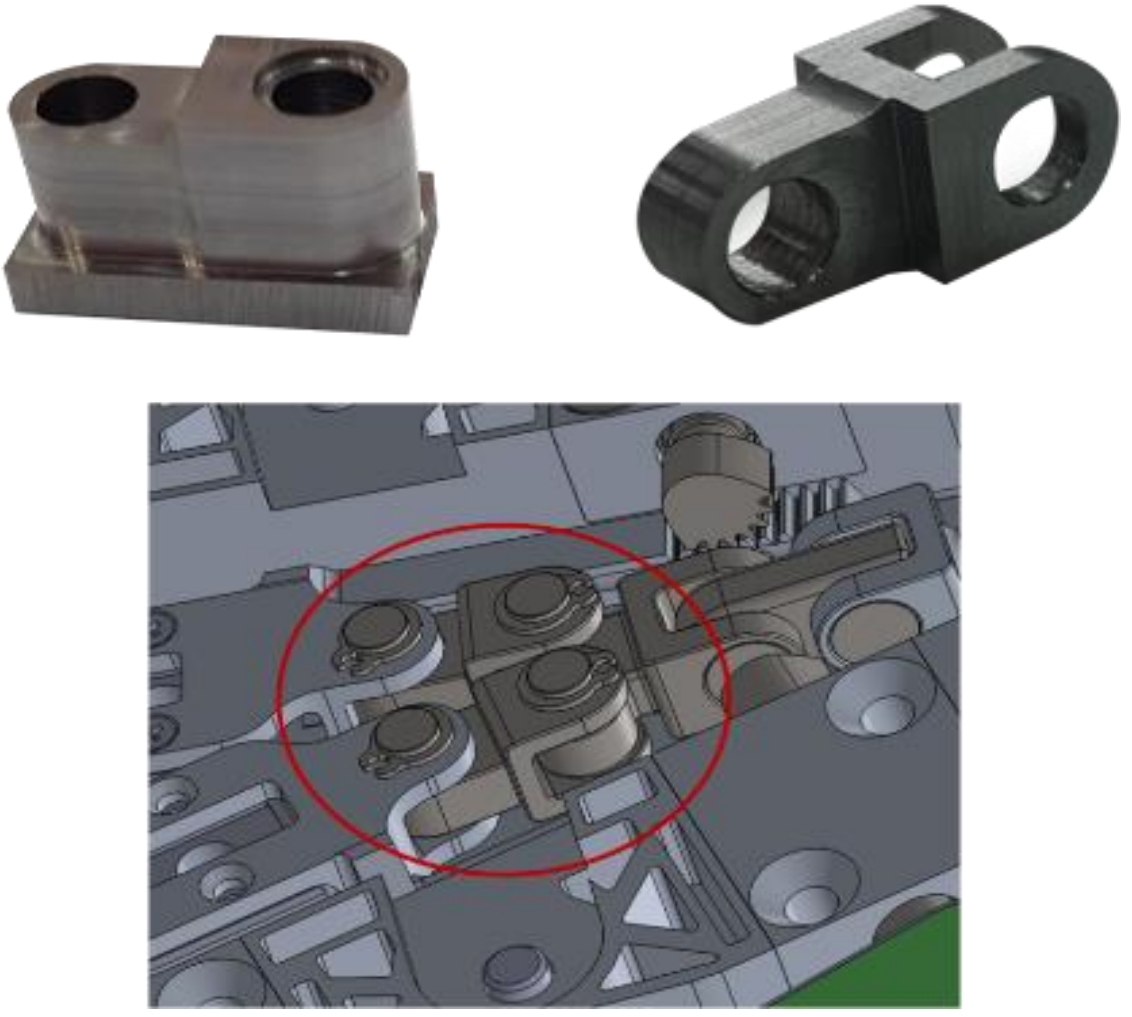

Fig. 19 CNC manufacturing of the connecting rod #1.

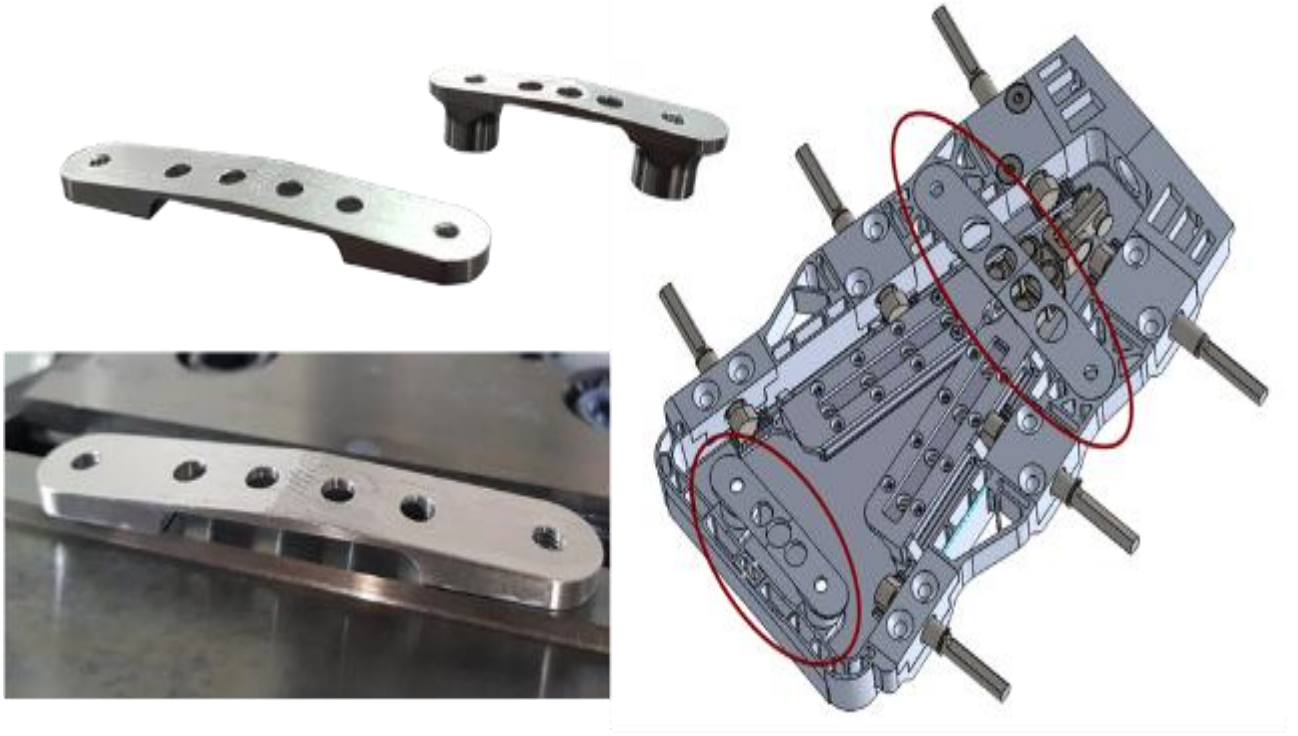

Fig. 20 CNC manufacturing of the fixing brackets on the crankcase.

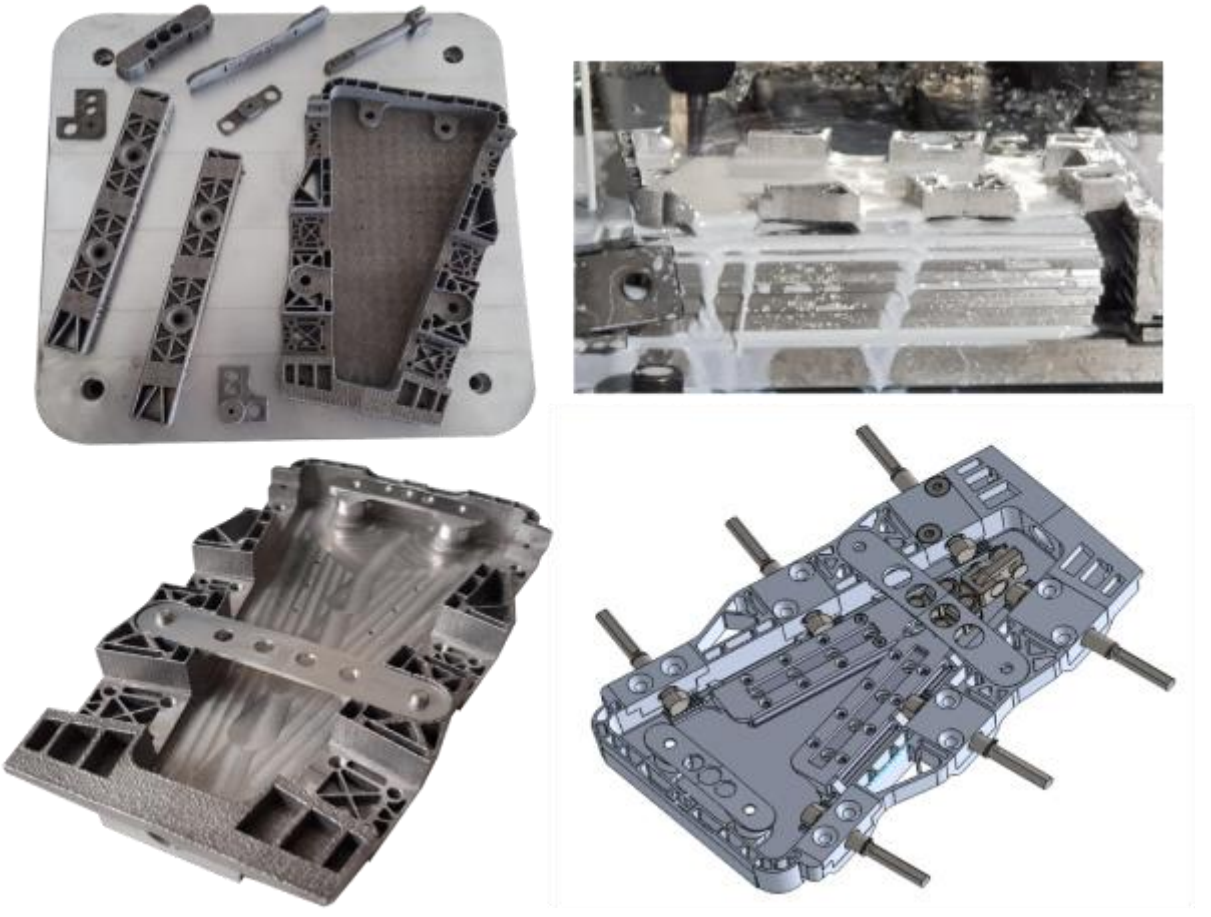

Fig. 21 ALM and CNC manufacturing of crankcase.

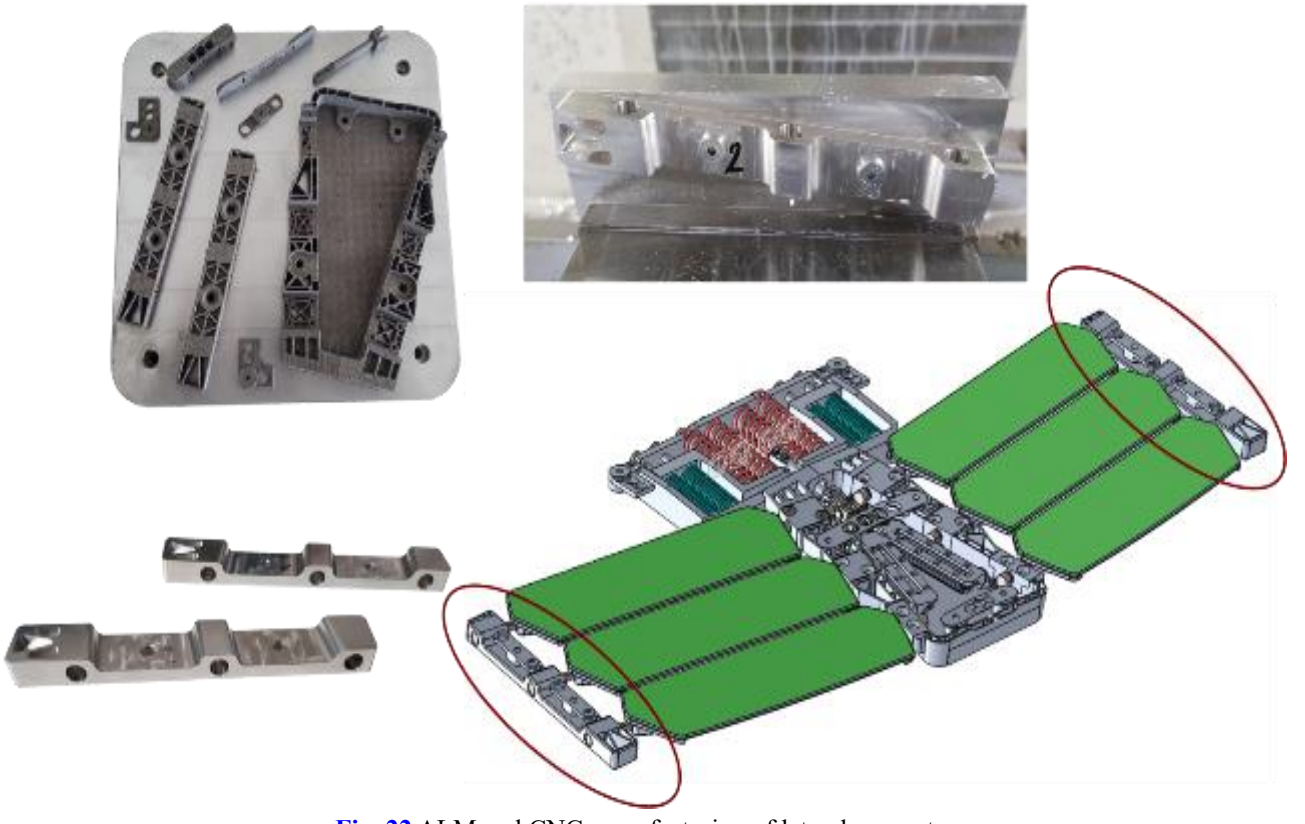

Fig. 22 ALM and CNC manufacturing of lateral supports.

It is worth to mention that, during the additive manufacturing process, particular attention has been paid to the arrangement and positioning of the manufacts on the manufacturing plate. The distance between the various components, the printing growth direction, the positioning of supports, the printing speed and the laser source intensity are fundamental parameters for the process. Indeed, improper positioning leads to printing failure or undesired deformation of the manufactured parts. To determine the best positioning of the components, several trials have been performed, as highlighted in Fig. 23. Indeed, Fig. 23a shows the inappropriate arrangement of the flap supports derived by an attempt to optimize the printing area without taking into account the components positioning influence on the output quality of the components selves. This wrong arrangement led to the failure of the structure due to residual internal stresses in four out of six printed components. The issue was solved by increasing the area and changing the positioning of the component on the manufacturing plate (Fig. 23b).

Fig. 23 Flap supports a) improperly and b) correctly printed.

6. Assembly and testing

In this section the assembly, calibration and testing activities performed on the SMA-based cooling system device to ensure its proper operational efficiency are described.

6.1 Assembly

The main steps followed to assembly the device can be summarised as follows:

Step 1: Kinematic parts assembly

The components have been installed on the crankcase in the following order:

- Gear racks (Fig. 24)
- Rotation rods with positioning blocks
- Connecting rod system

Fig. 24 Gear rack.

Step 2: Flaps supports and spring frame assembly

Once the kinematic parts assembly has been completed, the flap supports and the spring assembly frame have been assembled (Fig. 25).

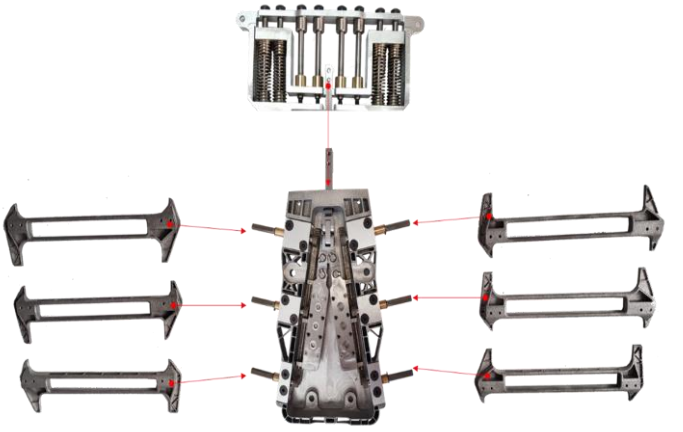

Fig. 25 Assembly scheme of the flap supports and the spring assembly frame.

Step 3: Side supports

Finally, the side supports have been installed on the device (Fig. 26).

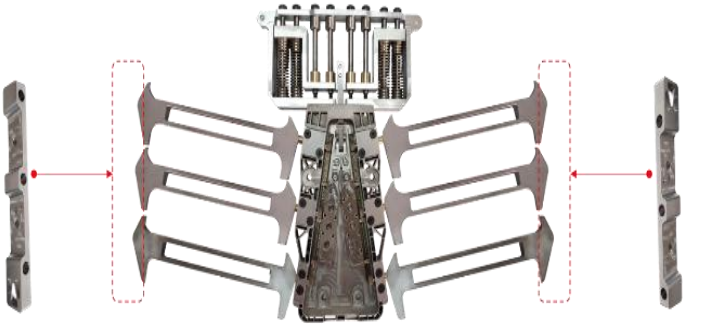

Fig. 26 Assembly scheme of the side supports.

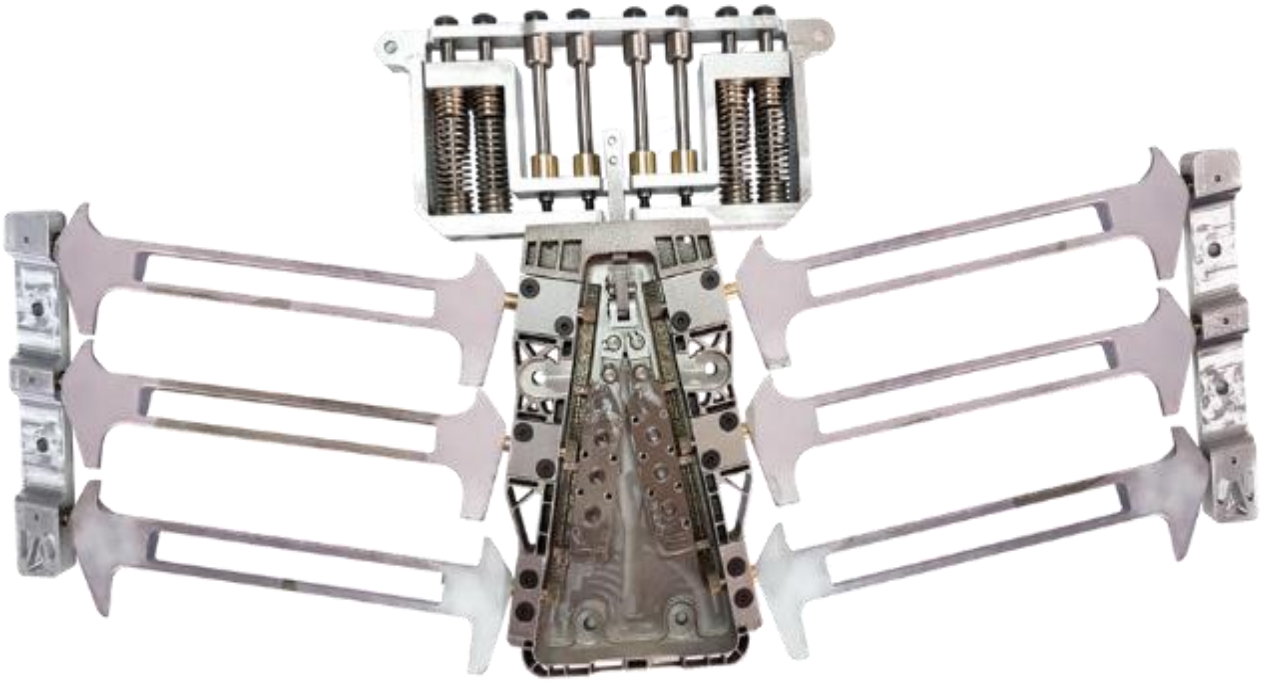

Fig. 27 Assembled SMA-based cooling system device.

The complete SMA-based cooling system device is reported in Fig. 27.

To integrate the SMA-based cooling system device on the Rear Bonnet, the supports shown in Fig. 28 have been fixed on the car structure by using high-strength structural Araldite (Fig. 29). In detail, the two-component glue Araldite 420 A/B, specific for the manufacture and processing of aramid materials, carbon fibres, and metal, has been used. Once the curing process of the resin was completed, the SMA cooling system have been accommodated and secured to its supports (Fig. 30). After the installation of the rear bonnet over the engine compartment, the Carbon PA Flaps have been glued on their supports.

Fig. 28 Supports.

6.2 Testing

To verify the proper operational effectiveness of the manufactured SMA-based cooling system device prototype, opening and closing operations have been performed in laboratory. To trigger and test the flaps opening mechanisms movement, a hot air flow has been applied onto the spring assembly by means of a hot gun to replicate the hot engine condition. This led to the activation of the SMA components and to the 60° rotation of the flaps, as expected (Fig. 31).

Similarly, liquid nitrogen was used to generate the cold air flow necessary to cool down the SMA components, resulting in flaps closure (Fig. 32). These operations have been repeated several times to understand the effects of friction on the opening and closing times.

Fig. 29 Supports glued on the rear bonnet.

Fig. 30 SMA-based cooling system device installed on the rear bonnet.

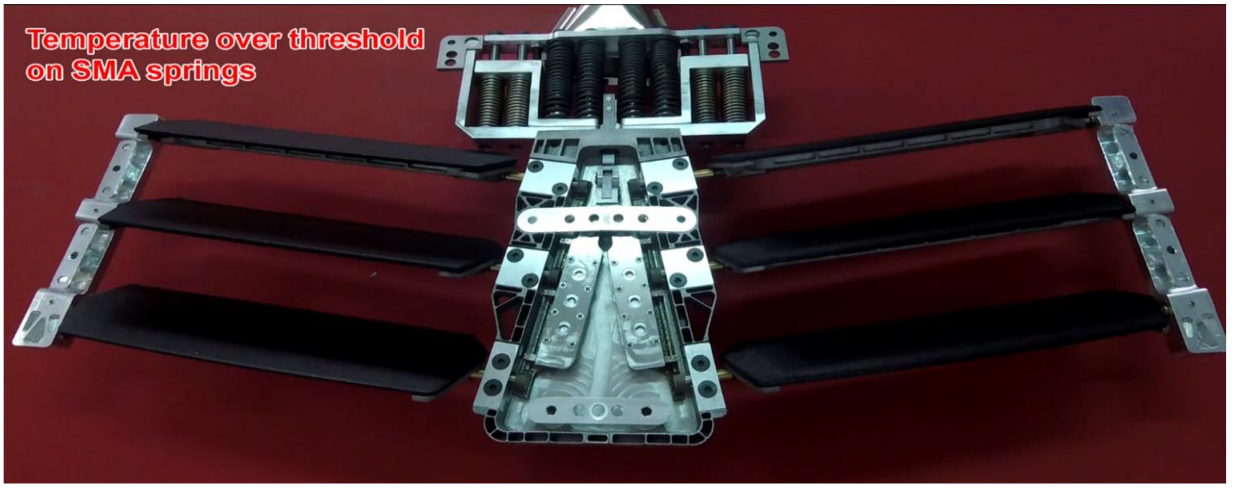

Fig. 31 SMA-based cooling system device opening test.

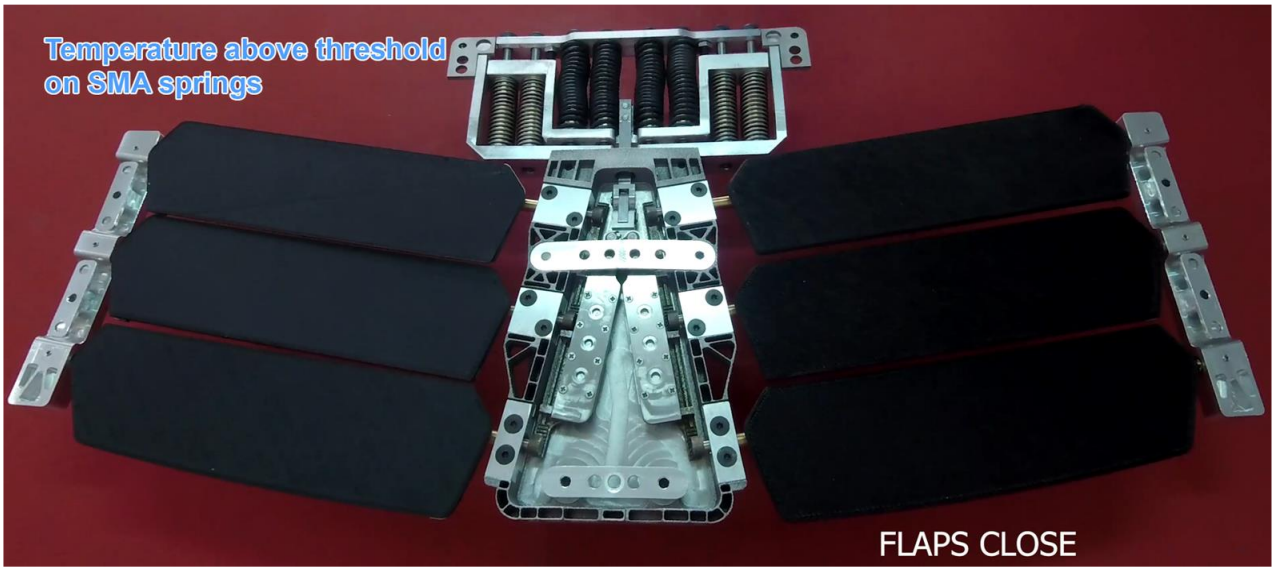

Fig. 32 SMA-based cooling system device closing test.

Finally, the passive cooling system has been mounted on the rear-bonnet of the Lamborghini Aventador S, and road tests have been performed (Fig. 33). The road tests, definitively, demonstrated the fulfilment of the requirements, in terms of actuation speed and actuation load. In particular, the aerodynamic forces due to the car movement did not affect the flaps, which remain in the open or closed configuration as required by the temperature conditions inside the engine compartment.

Fig. 33 SMA-based cooling system device: Road test.

7. Conclusions

In this work, the design and manufacturing steps for a SMA-based cooling system device has been presented. The Requirements, Preliminary Design, Executive Design, Manufacturing, Assembly and Testing activities have been introduced. The developed SMA system, designed to be integrated on the Rear-Bonnet of the Lamborghini Aventador S as test case, uses the peculiar characteristics of shape memory alloys to open rear flaps when a threshold activation temperature is reached in the engine compartment. This device, free from electronic control, can lower temperatures in the engine compartment allowing better performance and improving the operational life of the engine. Different manufacturing techniques, namely the Additive layer manufacturing and the Computerized Numerical Controlled Milling, have been used for the SMA based device components in order to maximize their weight reduction and to optimize their shape and volume.

The steps followed in manufacturing, pointing out the trial-and-error tests performed to optimize the process parameters, have been described in detail. The laboratory and road test performed on the developed SMA-based cooling system device, demonstrated its operational effectiveness.

Conflict of Interest

There is no conflict of interest.

Supporting Information

Not applicable.

References

[1] J. Qiu, C. Wang, C. Huang, H. Ji, Z. Xu, Smart skin and actuators for morphing structures, *Procedia IUTAM*, 2014, **10**, 427-441, doi: 10.1016/j.piutam.2014.01.037.

[2] J. Bowman, B. Sanders, B. Cannon, J. Kudva, S. Joshi, T. Weisshaar, Collection of technical papers - AIAA/ASME/ASCE/AHS/ASC Structures, *Structural Dynamics and Materials Conference*, 2007, **1**, 349-358, doi: 10.2514/6.2007-1730

[3] A. Sellitto, A. Riccio, Overview and future advanced engineering applications for morphing surfaces by shape memory alloy materials, *Materials*, 2019, **12**, 708, doi: 10.3390/ma12050708.

[4] T. A. Weisshaar, D. K. Duke, Induced drag reduction using aeroelastic tailoring with adaptive control surfaces, *Journal of Aircraft*, 2006, **43**, 157-164, doi: 10.2514/1.12040.

[5] D. A. Perkins, J. L. Reed Jr., E. Havens, Adaptive wing structures, *Proceedings of SPIE - The International Society for Optical Engineering*, 2004, **5388**, 225-233, doi: 10.1117/12.541650.

[6] C. Nam, A. Chattopadhyay, Y. Kim, Application of shape memory alloy (SMA) spars for aircraft manoeuvre enhancement, *Proceedings of SPIE - The International Society for Optical Engineering*, 2002, 226-237, doi: 10.1117/12.474661.

[7] S.-H. Hwang, H. W. Park, Y.-B. Park, Piezoresistive behavior and multi-directional strain sensing ability of carbon nanotube-graphene nanoplatelet hybrid sheets, *Smart Materials and Structures*, 2013, **22**, 015013, doi: 10.1088/0964-1726/22/1/015013.

[8] Y. Hou, R. Neville, F. Scarpa, C. Remillat, B. Gu, M. Ruzzene, Graded conventional-auxetic Kirigami sandwich structures: Flatwise compression and edgewise loading, *Composites Part B: Engineering*, 2014, **59**, 33-42, doi: 10.1016/j.compositesb.2013.10.084.

[9] T. Schmelter, B. Theren, S. Fuchs, B. Kuhlenkötter, Development of an actuator for translatory movement by means of a detented switching shaft based on a shape memory alloy wire for repeatable mechanical positioning, *Crystals*, 2021, **11**, 163, doi: 10.3390/cryst11020163.

[10] E. Ayvali, J. P. Desai, Pulse width modulation–based temperature tracking for feedback control of a shape memory alloy actuator, *Journal of Intelligent Material Systems and Structures*, 2014, **25**, 720-730, doi: 10.1177/1045389X13502576.

[11] C. Thill, J. Etches, I. Bond, K. Potter, P. Weaver, Morphing skins, *The Aeronautical Journal*, 2008, **112**, 117-139, doi: 10.1017/s0001924000002062.

[12] S. Barbarino, O. Bilgen, R. M. Ajaj, M. I. Friswell, D. J. Inman, A review of morphing aircraft, *Journal of Intelligent*

Material Systems and Structures, 2011, **22**, 823-877, doi: 10.1177/1045389x11414084.
[13] J. Mohd Jani, M. Leary, A. Subic, M. A. Gibson, A review of shape memory alloy research, applications and opportunities, *Materials & Design*, 2014, **56**, 1078-1113, doi: 10.1016/j.matdes.2013.11.084.
[14] J. Mohd Jani, M. Leary, A. Subic, Designing shape memory alloy linear actuators: a review, *Journal of Intelligent Material Systems and Structures*, 2017, **28**, 1699-1718, doi: 10.1177/1045389x16679296.
[15] Z. Khoo, J. An, C. Chua, Y. Shen, C. Kuo, Y. Liu, Effect of heat treatment on repetitively scanned SLM NiTi shape memory alloy, *Materials*, 2018, **12**, 77, doi: 10.3390/ma12010077.
[16] W. Wang, H. Rodrigue, S.-H. Ahn, Smart soft composite actuator with shape retention capability using embedded fusible alloy structures, *Composites Part B: Engineering*, 2015, **78**, 507-514, doi: 10.1016/j.compositesb.2015.04.007.
[17] L. Brinson, One-Dimensional Constitutive Behavior of Shape Memory Alloys: Thermomechanical Derivation with Non-Constant Material Functions and Redefined Martensite Internal Variable, *Journal of Intelligent Material Systems and Structures*, 1993, **4**, 229-242, doi: 10.1177/1045389X93004002.
[18] J. Van Humbeeck, Shape memory alloys: a material and a technology, *Advanced Engineering Materials*, 2001, **3**, 837, doi: 10.1002/1527-2648(200111)3: 11837: aid-adem837>3.0.co;2-0.
[19] A. Osorio Salazar, Y. Sugahara, D. Matsuura, Y. Takeda, A Novel, Scalable Shape Memory Alloy Actuator Controlled by Fluid Temperature, *Mechanisms and Machine Science*, 2021, **91**, 617-625, doi: 10.1007/978-3-030-55807-9_69.
[20] S. Akbari, A. H. Sakhaei, S. Panjwani, K. Kowsari, Q. Ge, Shape memory alloy-based 3D printed composite actuators with variable stiffness and large reversible deformation, *Sensors and Actuators A: Physical*, 2021, **321**, 112598, doi: 10.1016/j.sna.2021.112598.
[21] T. Chen, J. Jiang, Q. Zhang, H. Wang, X. Zhang, Experiments and modeling of variable camber guide vane embedded with shape memory alloy plate, *Smart Materials and Structures*, 2021, **30**, 045012, doi: 10.1088/1361-665x/abe846.
[22] N. Simiriotis, M. Fragiadakis, J. F. Rouchon, M. Braza, Shape control and design of aeronautical configurations using shape memory alloy actuators, *Computers & Structures*, 2021, **244**, 106434, doi: 10.1016/j.compstruc.2020.106434.
[23] A. Concilio, S. Ameduri, Influence of structural architecture on linear shape memory alloy actuator performance and morphing system layout optimisation, *Journal of Intelligent Material Systems and Structures*, 2014, **25**, 2037-2051, doi: 10.1177/1045389x13517306.
[24] A. Riccio, A. Sellitto, A. Caraviello, U. Riccio, A. Torluccio, L. Pacini, R. Mohr, S. H. Tech via Romani Sant'Anastasia (NA) Italy, On the development of a passive shape memory alloy-based cooling system - part II: design justification, *Engineered Science*, 2023, doi: 10.30919/es928.
[25] P. Shayanfard, L. Heller, P. Šandera, P. Šittner, Numerical analysis of NiTi actuators with stress risers: the role of bias load and actuation temperature, *Engineering Fracture Mechanics*, 2021, **244**, 107551, doi: 10.1016/j.engfracmech.2021.107551.
[26] V. E. Liete Gasparetto, M. Kanevsky, X. X. Jiang, Solar Panel Deployment Using Shape Memory Alloy Actuator, *AIAA Scitech 2021 Forum*, 2021, 1608, doi: 10.2514/6.2021-1608.